The decomposition of NO on CNTs and 1 wt% Rh/CNTs

J.Z. Luo [a], L.Z. Gao [a,b], Y.L. Leung [c] and C.T. Au [a,*]

[a] *Department of Chemistry, Hong Kong Baptist University, Kowloon Tong, Hong Kong, PR China*
E-mail: pctau@hkbu.edu.hk
[b] *Chengdu Institute of Organic Chemistry, Chinese Academy of Sciences, Chengdu, Sichuan, 610041, PR China*
[c] *Department of Physics, Hong Kong Chinese University, NT, Hong Kong, PR China*

Received 10 December 1999; accepted 20 March 2000

Carbon nanotubes (CNTs) and CNTs-supported rhodium were tested as catalysts for NO decomposition. For the fresh catalysts, 100% NO conversion was achieved at 600 °C over CNTs; when 1 wt% Rh was loaded on CNTs, 100% NO conversion was achieved at 450 °C. If the catalysts were pre-reduced in H_2 at or above 300 °C, 100% NO conversions were observed at 300 °C. XPS investigation indicated that there was still metallic rhodium (BE = 307.2 eV) on Rh/CNTs after heating in air at 500 °C for 2 h and after the NO decomposition reaction. As for a 1 wt% Rh/Al_2O_3 sample, the rhodium (BE = 308.2 eV) was completely in the form of Rh_2O_3 after similar treatments. These results suggest that compared to γ-Al_2O_3, the CNTs material is more capable of keeping the rhodium in its metallic state. The results obtained in H_2-TPR studies support this conclusion. In addition, TEM investigation revealed that the rhodium particles distributed rather evenly over CNTs with a particle diameter of around 8 nm. We propose that CNTs can be used as a material for the facilitation of NO decomposition.

Keywords: carbon nanotubes (CNTs), CNTs-supported rhodium catalysts, NO decomposition

1. Introduction

Carbon nanotubes (CNTs) are hollow nano-size tubes of concentric graphitic carbon capped by fullerene-like hemispheres. The material possesses unique electronic and structural properties [1] as well as strong hydrogen storage ability [2,3]. These properties enable the CNTs to be potential catalytic materials. Up to now, the application of CNTs in heterogeneous catalysis is still in its infancy [4]. In the liquid-phase hydrogenation of cinnamaldehyde, Planeix et al. [5] reported that CNTs-supported ruthenium and platinum catalysts were more durable and showed higher selectivity in cinnamyl alcohol as compared to the graphite- and Al_2O_3-supported ones. Similar promotion effects of CNTs were also observed in the hydrogenation of CO and 2-cyclohexenone [6,7].

The generation of nitrogen oxides in the combustion of coals and other nitrogen-containing fuels remains as a problem of considerable interest due to the contribution of these pollutants to rain acidification, global warming, and the depletion of the stratospheric ozone layer [8,9]. Generally speaking, there are four methods to eliminate NO_x: (1) the selective catalytic reduction of NO_x with ammonia; (2) the catalytic reduction of NO_x in the presence of CO and/or H_2; (3) the selective catalytic reduction of NO_x in the presence of hydrocarbons; and (4) the direct decomposition of NO_x. Among the methods, the fourth one is the most attractive for it needs no reductants and NO_x decomposes directly into O_2 and N_2. Although numerous investigations on NO decomposition have been conducted, e.g., [10,11], no suitable catalyst with sustainable activity has been found. It has been suggested that catalyst deactivation might be due to the strong surface adsorption of the oxygen atoms generated in NO dissociation [12].

In this report, CNTs and CNTs-supported rhodium were investigated for NO decomposition. Rhodium was used for it is widely recognized as an active component to catalyze the reduction of NO [11,13–15]. The oxidation state of noble metal in a catalyst has direct influence on the catalytic performance. For instance, Pisanu and Gigola [16] pointed out that the active centres for NO decomposition was metallic Pd^0 rather than Pd^{2+}. Our results of TEM, TPR, and XPS studies revealed that the presence of CNTs is favourable for the retention of metallic rhodium and the catalytic activity of rhodium is enhanced as a result.

2. Experimental

The CNTs were synthesized *in situ* by means of CO disproportionation as previously described [17]. We exposed the H_2-reduced Ni–La_2O_3/5A catalyst to a flow of CO (10 ml min^{-1}) at 600 °C for 30 min. The CNTs had been treated in 1 M HNO_3 and washed with deionized water. According to the TEM images, after two HNO_3 treatments, there were only CNTs and amorphous carbon. The samples were then subjected to toluene extraction and air oxidation (500 °C for 2 h) for the removal of amorphous carbon. These purification procedures would result in CNTs of high purity. The yield of CNTs was about 100 g/g_{Ni}. In TEM investigation, no materials other than CNTs were observed [17,18].

* To whom correspondence should be addressed.

CNTs-supported rhodium was prepared by impregnating CNTs with a 5 mM $RhCl_3{\cdot}3H_2O$ solution. After impregnation, the material was dried at 80 °C and then calcined at 500 °C in air for 2 h, respectively. The loading of Rh in the Rh/CNTs obtained was 1 wt%. For comparison, we also prepared 1 wt% Rh/γ-Al_2O_3 according to the procedures described but using γ-Al_2O_3 as the support.

Activity evaluations were carried out in a quartz tube microreactor (i.d. = 4 mm) by pulsing NO (purity = 99%) into the reactor with He (purity = 99.999%, 10 ml min^{-1}) being the carrier gas. The sample (10 mg) was placed in the middle of the reactor between two quartz wool plugs. The reaction temperature was regulated from 300 to 700 °C. The size of each pulse was 67.5 μl. The blank runs conducted with only quartz wool plugs in the reactor indicated that without the catalyst, the decomposition of NO up to 700 °C was negligible. The effluent gases were monitored on line by a mass spectrometer (HP G-1800A). For quantitative analysis of products, we adopted 5A and Porapak Q columns to separate N_2 ($m/z = 28$), N_2O ($m/z = 44$), CO ($m/z = 28$), and CO_2 ($m/z = 44$).

The TPR experiment was carried out by using a 7% H_2–93% N_2 (v/v) gas mixture. The flow rate was 50 ml min^{-1} and a thermal conductivity detector was employed. The amount of sample was 10 mg and the heating rate was 10 °C min^{-1}. Before performing a TPR experiment, the sample was first calcined *in situ* at 300 °C for 1 h in an O_2 flow of 15 ml min^{-1} followed by cooling in O_2 to room temperature and purging with the carrier gas for 20 min.

The CO chemisorption experiments were performed in a quartz microreactor (i.d. = 4 mm). The sample (10 mg) was first treated in H_2 (10 ml min^{-1}) at 300 °C for 1 h, followed by cooling in H_2 to room temperature and He purging for 10 min. We kept on pulsing CO to the catalyst until there was no observable increase in CO signal intensity. The uptake of CO was then estimated and was used to calculate Rh metal dispersion and particle size, assuming that each surface metal atom chemisorbs one CO molecule, i.e., $CO/Rh_{surface} = 1$.

The specific surface areas of the catalysts were measured by the BET method using a NOVA-1200 instrument. TEM images were taken by means of a JEM-100 CX (Jeol) equipment operated at 50 kV at room temperature. The sample was dispersed by ultrasonic bath of aqueous surfactant solution before mounting on a Cu grid for TEM observation. XPS experiments were conducted on a Kratos surface analyzer (AXIS HS) at room temperature. The C_{1s} binding energy (284.6 eV) of carbonaceous matter was adopted for internal calibration.

3. Results

3.1. Physico-chemical properties

Some physico-chemical properties of the catalysts are listed in table 1. The CNTs showed a specific surface area of 180 $m^2\,g^{-1}$. Loading Rh (1 wt%) onto CNTs reduced the specific surface area to 140 $m^2\,g^{-1}$. The CNTs material exhibits affinity to CO; the CO uptake at room temperature was 22 μmol g^{-1}. The presence of metallic rhodium on CNTs enhanced CO adsorption; CO uptake was 60 μmol g^{-1}. For the 1 wt% Rh/CNTs catalyst, the particle size of metallic Rh was estimated to be 10.7 nm according to CO chemsorption data, a value rather close to that (5–10 nm) of the TEM image. Although the surface area of 1 wt% Rh/γ-Al_2O_3 (120 $m^2\,g^{-1}$) was similar to that of 1 wt% Rh/CNTs (140 $m^2\,g^{-1}$), CO uptake (25 μmol g^{-1}) of the former was significantly lower than that of the latter (60 μmol g^{-1}). The diameter of the rhodium particles on Rh/γ-Al_2O_3 as estimated by CO chemisorption was around 25.7 nm.

3.2. Catalytic performance for NO decomposition

3.2.1. Over fresh catalysts

Figure 1 shows the variation of catalytic activity as related to reaction temperature observed over the fresh CNTs, 1 wt% Rh/CNTs, and 1 wt% Rh/γ-Al_2O_3 catalysts. Besides N_2 and O_2, N_2O was also observed as a product. NO_2 was not detected in the effluent gases under our experimental conditions. For CNTs, the conversion of NO was 8.0% at 300 °C and increased with temperature rise. Between 500 and 600 °C, there was a rapid increase in NO conversion, and nearly 100% NO conversion was observed at or above 600 °C. For 1 wt% Rh/CNTs, a NO conversion of 10% was observed at 300 °C. There was a linear increase in NO conversion between 300 and 400 °C; nearly 100% NO conversion was achieved at or above 450 °C. Among the three catalysts, 1 wt% Rh/γ-Al_2O_3 showed the lowest activity: NO conversion was ca. 5% at 300 °C and increased gradually with the rise in reaction temperature; at 700 °C, NO conversion was only ca. 54%. Figures 2 and 3 show

Table 1
Physico-chemical properties of CNTs, Rh/CNTs, and Rh/γ-Al_2O_3.

Catalyst	Surface area ($m^2\,g^{-1}$)	CO uptake (μmol g^{-1})	Dispersion (%)	Metallic particle size (nm)	
				[a]	[b]
CNTs	180	22	–	–	–
1 wt% Rh/CNTs	140	60	62.7	10.7	5–10
1 wt%Rh/γ-Al_2O_3	120	25	26.1	25.7	–

[a] Based on data obtained in CO adsorption at room temperature.
[b] Based on TEM images.

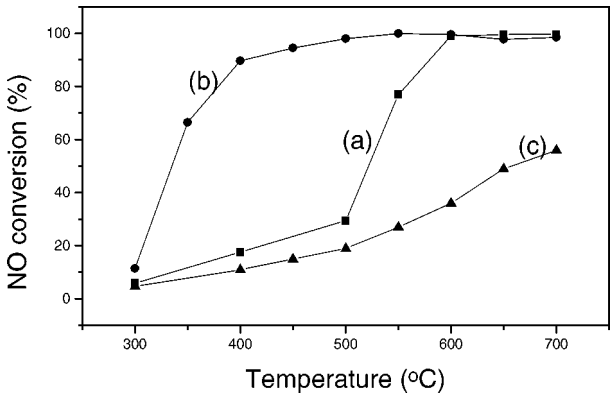

Figure 1. NO conversion versus reaction temperature over fresh (a) CNTs, (b) 1 wt% Rh/CNTs, and (c) 1 wt% Rh/γ-Al_2O_3.

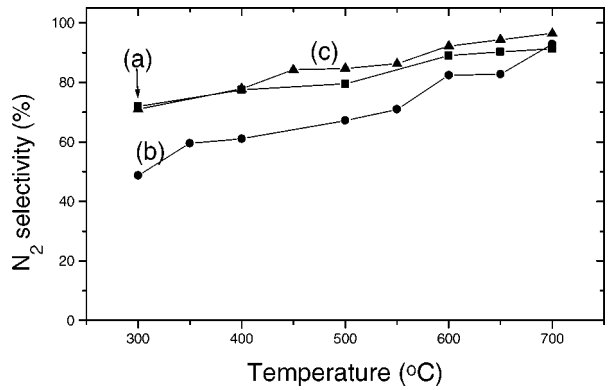

Figure 2. N_2 selectivity versus reaction temperature over fresh (a) CNTs, (b) 1 wt% Rh/CNTs, and (c) 1 wt% Rh/γ-Al_2O_3.

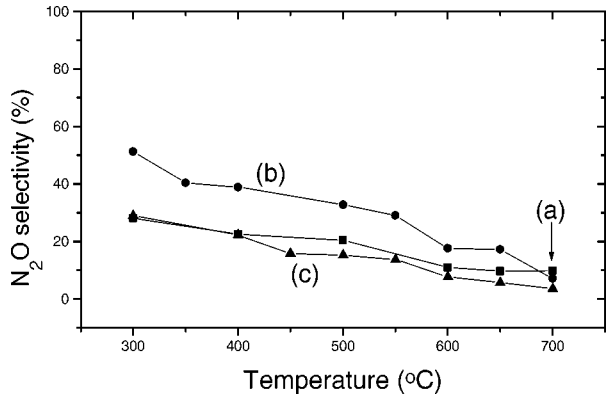

Figure 3. N_2O selectivity versus reaction temperature over fresh (a) CNTs, (b) 1 wt% Rh/CNTs, and (c) 1 wt% Rh/γ-Al_2O_3.

the selectivities of N_2 and N_2O, respectively, over fresh CNTs, 1 wt% Rh/CNTs, and 1 wt% Rh/γ-Al_2O_3. Compared to CNTs, the Rh/CNTs catalyst is more favourable for the production of N_2O; the N_2O selectivity observed over the latter was constantly higher than that observed over the former. The tendency of N_2 formation increased whereas that of N_2O formation decreased with the rise in reaction temperature.

Figure 4 shows the amount of CO_2 produced in a pulse of NO as a function of reaction temperature over CNTs and

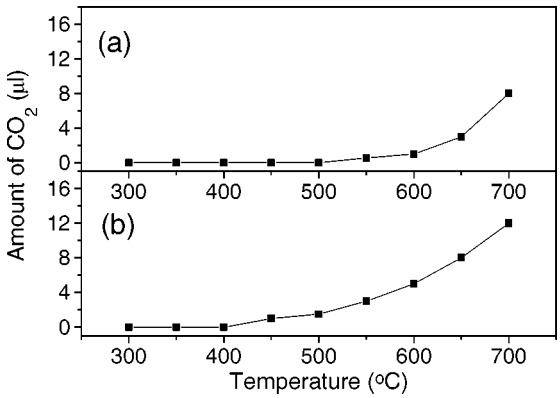

Figure 4. The amount of CO_2 produced in a NO pulse versus reaction temperature over (a) CNTs and (b) 1 wt% Rh/CNTs. The size for each pulse was 67.5 μl.

1 wt% Rh/CNTs. The detection of CO_2 in the effluent indicated the involvement of CNTs in NO decomposition. For CNTs (figure 4(a)), one can note that CO_2 is only generated at or above 500 °C. At temperatures higher than 500 °C, the amount of CO_2 produced increases with the rise in reaction temperature. Similar tendency was observed over 1 wt% Rh/CNTs (figure 4(b)). The threshold temperature for CO_2 generation is 400 °C, then with the increase of reaction temperature, the amount of CO_2 in the effluent increases.

3.2.2. Over H_2-reduced catalysts

Table 2 lists the amount of NO consumed at 300 °C in ten pulses of NO over the reduced CNTs, Rh/CNTs, and Rh/γ-Al_2O_3 catalysts. Each catalyst was pretreated *in situ* with H_2 at a desired temperature. In the first pulse, NO consumption was 100% and N_2 was the only detected product. With the rise in pulse number, we observed that the NO conversion decreased gradually and then leveled off after ten pulses; the selectivity for N_2 production decreased while that for N_2O formation increased. It can be observed that with the rise in the temperature adopted for H_2-treatment, the amount of NO converted at 300 °C increased. Over H_2-treated (300 °C, 1 h) CNTs, the NO conversion in the tenth pulse was ca. 8% and totally 90.0 μl NO was converted in ten NO pulses. The addition of 1 wt% rhodium onto CNTs improved the catalytic performance greatly. The NO conversion in the tenth pulse was ca. 21%; the total amount of NO converted over a 300 °C-reduced 1 wt% Rh/CNTs was 418.1 μl, about 4.5 times that of CNTs. The 1 wt% Rh/γ-Al_2O_3 catalyst was inferior to 1 wt% Rh/CNTs in performance and the NO conversion in the tenth pulse was 12%; totally, only 136.2 μl of NO was converted in ten pulses of NO over the 300 °C-reduced sample.

3.3. Catalyst characterization

3.3.1. TEM

Figure 5 shows the TEM images of CNTs and 1 wt% Rh/CNTs. The CNTs are highly crystalline; the outer diameter is in the range of 10–30 nm and the inner diameter is about 1 nm (figure 5(a)). There were no other mate-

Table 2
The amount (μl) of NO converted at 300 °C in ten pulses of NO over the catalysts treated in H_2 for 1 h at various temperatures. Also shown are the NO conversions in the tenth NO pulse over the catalysts which had been treated in H_2 for 1 h at 300 °C, respectively.

Catalyst	Reduction temperature (°C)					NO conversion in
	300	400	500	600	700	the tenth pulse (%)
CNTs	90.0	94.7	96.7	100.0	122.0	8.0
1 wt% Rh/CNTs	418.1	437.7	468.4	479.0	482.3	21.0
1 wt% Rh/γ-Al_2O_3	136.2	152.1	165.4	166.3	148.2	12.0

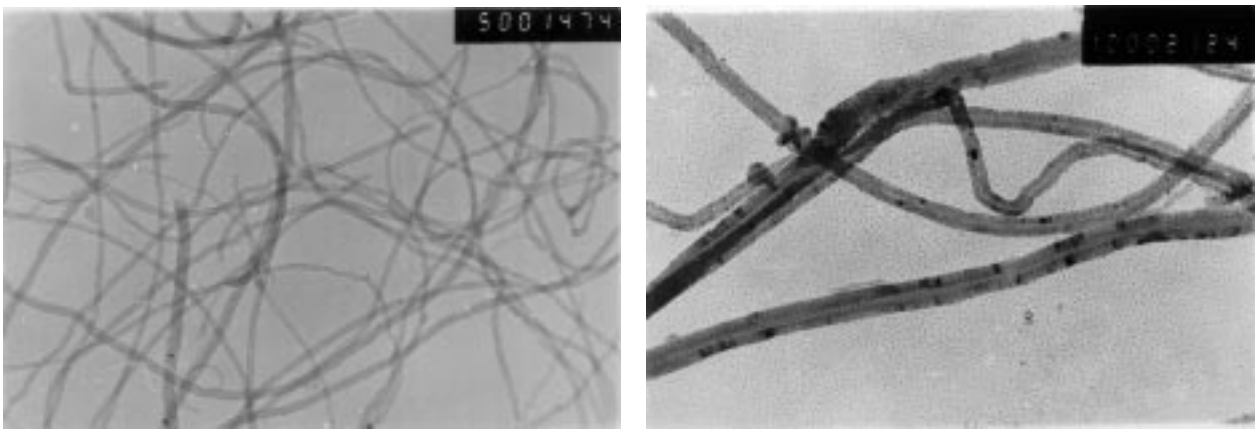

(a) (b)

Figure 5. TEM images of (a) CNTs and (b) 1 wt% Rh/CNTs.

rials co-existing with CNTs. The dark spots observed in figure 5(b) are assigned to rhodium particles. It is apparent that rhodium disperses mostly on the surface of CNTs.

3.3.2. XPS

Figure 6 shows the Rh_{3d} XPS spectra of 1 wt% Rh/CNTs and 1 wt% Rh/γ-Al_2O_3. The peaks centered at 307.2 and 308.3 eV (binding energy) are attributed to metallic Rh^0 and Rh_2O_3, respectively [19]. For a fresh Rh/CNTs sample, the result of curve-fitting indicated clearly that rhodium existed predominantly (80%) in the Rh_2O_3 form, with the rest being metallic. After treatment in H_2 at 300 °C for 2 h, most of the Rh_2O_3 was reduced to the metallic state. For a sample used in NO decomposition at 700 °C, the relative ratio of Rh^0/Rh^{3+} was about 3/10. For comparison, the rhodium in the fresh and used Rh/γ-Al_2O_3 samples existed exclusively in the form of Rh_2O_3; even after H_2-reduction at 300 °C for 1 h, 45% of the rhodium still existed as Rh_2O_3.

3.3.3. TPR experiments

Figure 7 shows the TPR profiles of CNTs, 1 wt% Rh/CNTs, and 1 wt% Rh/γ-Al_2O_3. For CNTs, there is one peak which rises at 180 °C and centers at 300 °C. This peak can be assigned to the hydrogenation of active carbonaceous species in CNTs [3]. The loading of 1 wt% Rh on CNTs results in a large increase in H_2 consumption and the TPR peak area is about eight times bigger than that of CNTs. The peak rises at ca. 60 °C and reaches an apex at ca. 280 °C. We suggest that the large consumption of H_2 was due to the reduction of Rh_2O_3 to metallic rhodium as well as the hydrogenation of CNTs support. The apex of the TPR peak of Rh/γ-Al_2O_3 is at 350 °C, 70 °C higher than that observed over Rh/CNTs. The TPR peak area of Rh/γ-Al_2O_3 was about half that of Rh/CNTs. Apparently, compared to the Rh_2O_3 of Rh/γ-Al_2O_3, the Rh_2O_3 of Rh/CNTs is more likely to be reduced to Rh^0.

4. Discussion

It is generally believed that the decomposition of NO follows the redox mechanism [9,11,20]:

$$M^{n+} \rightleftharpoons M^{(n+1)+} + e$$
$$NO + e \rightleftharpoons NO^-$$

where M is a metal and $n = 0$, 1 or 2. Subsequently, the adsorbed NO^- can decompose to N_2 and O_2 via intermediates such as $N_2O_2^{2-}$ and NO_2^-. In the reaction, M^{n+} serves as the active sites. If the recovery of M^{n+} from $M^{(n+1)+}$ is not timely, $M^{(n+1)+}$ would accumulate. As a result, the conversion of NO was hindered. The strong interactions between metal and carbon support have been extensively studied. Braun et al. pointed out that η^2-type metal–carbon bonds could be formed in fullerene-based ruthenium catalysts [6,7]. The presence of fullerenes should therefore cause an interaction between the metal and the substrate, one that is different from the interaction of conventional carbon materials with metal particles. Similar viewpoints have also been made on CNTs materials [21]. From figure 1, one can observe that 1 wt% Rh/CNTs exhibits higher

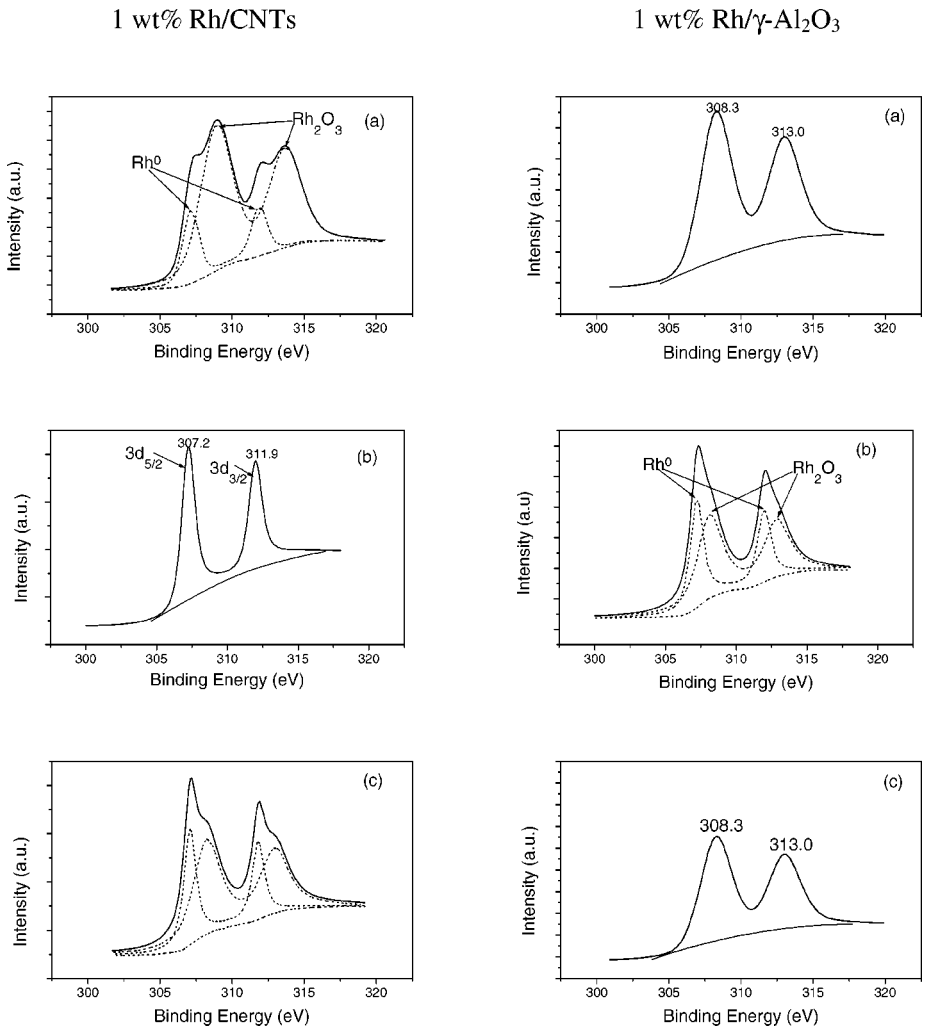

Figure 6. XPS spectra of 1 wt% Rh/CNTs and 1 wt% Rh/γ-Al_2O_3: (a) fresh, (b) after H_2 treatment at 300 °C, and (c) after the NO decomposition reaction.

activity for NO decomposition than pure CNTs and 1 wt% Rh/γ-Al_2O_3. Therefore, we envision that within a CNTs-supported metal catalyst, the transfer of electrons from CNTs to $M^{(n+1)+}$ would facilitate the recovery of M^{n+}. In other words, there is a larger amount of metallic Rh present on the 1 wt% Rh/CNTs catalyst and the interaction of CNTs with the metal would enhance electron backfeeding from the metal to the anti-bonding orbital of NO, facilitating the breaking of N–O bond as a result. In addition, a NO may obtain an electron from CNTs directly to become NO^-. The results would be the enhancement in NO activation.

Fresh CNTs showed moderate activity for NO decomposition (figure 1). The detection of CO_2 as a product indicated that the oxygen derived from NO decomposition was active enough to oxidize CNTs under these reaction conditions. The oxidative reaction was more significant at or above 500 °C (figure 4). These results indicated that CNTs served as a catalyst below 500 °C and as a reducing agent above 500 °C. This is in line with the observation of Illán-Gómez et al. [22], who investigated the catalytic reduction of NO over carbon-supported metals (Fe, Co, Ni, and Cu) and found that the carbon support could reduce NO. Compared to fresh CNTs, the CNTs pretreated with H_2 showed much better catalytic activity. The temperature to achieve 100% NO conversion to N_2 was lowered by 300 °C if CNTs were first treated by H_2 at 300 °C for 1 h. Totally, ca. 90 μl of NO was converted in ten NO pulses (table 2). Over fresh CNTs, the total amount of NO converted was 54.0 μl. Since there was no metal involved, the difference (i.e., 36 μl) must be predominantly due to the presence of H species in the CNTs. In TPR experiment we observed a H_2-consuming peak at ca. 300 °C (figure 7(a)). Generally speaking, H uptake might be due to the intercalation and adsorption of hydrogen as well as the hydrogenation of CNTs. It is known that CNTs have the ability for H_2 storage [2,3]. However, considering the high temperature (300 °C), we propose that the TPR peak at 300 °C is due to CNTs hydrogenation rather than H_2 adsorption. This suggestion is in line with the IR results reported by Chen et al.; they observed the gradual increase of C–H vibration signal with H_2-exposure time over CNTs at 377 °C [3]. In addition, the NO conversion (8.0%) in the tenth pulse of NO over H_2-reduced CNTs was similar

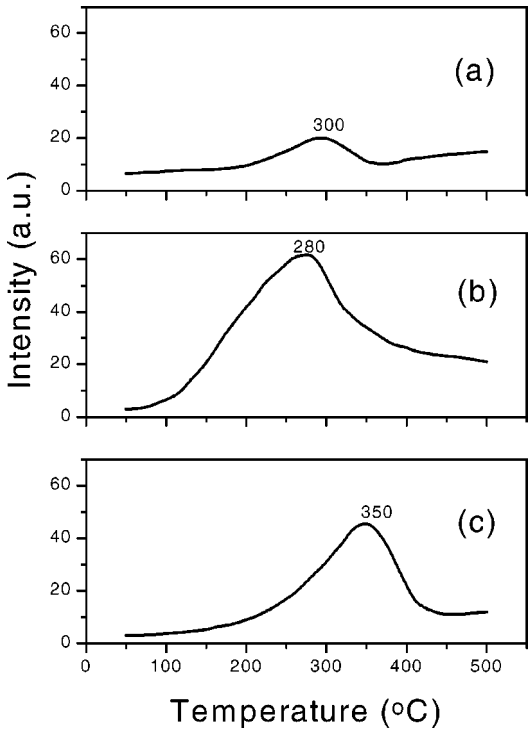

Figure 7. TPR profiles of (a) CNTs, (b) 1 wt% Rh/CNTs, and (c) 1 wt% Rh/γ-Al_2O_3.

to that observed over a fresh sample (figure 1). This result revealed that the H species over CNTs are active enough to participate in the activation of NO. With the rise in pulse number, the amount of H species decreased gradually to complete consumption, and NO conversion decreased to a value similar to that observed over a fresh sample. From table 2, it can be observed that the amount of NO consumed increased moderately with the rise in the temperature for H_2 treatment. We speculate that at higher treatment temperature, more hydrogen were retained in CNTs and NO decomposition was enhanced as a result.

The TEM image in figure 5(b) illustrates the homogeneity of the rhodium particles over 1 wt% Rh/CNTs. The particle size (5–10 nm) estimated from the TEM image and that (10.7 nm) calculated according to the CO chemisorption data are in good agreement. The homogeneity and the small size of rhodium particles indicate that CNTs can disperse Rh and the material can be used as a support for rhodium-based catalysts. We observed ca. 100% NO conversion at ca. 450 °C over fresh 1 wt% Rh/CNTs, about 150 °C lower than that observed over fresh CNTs (figure 1). XPS investigation revealed that ca. 30% of rhodium existed as metal over the used Rh/CNTs catalyst (figure 6(c)). The co-existence of metallic rhodium and Rh_2O_3 reveals the redox mechanism of NO decomposition [12,13]. The retention of a certain amount of metallic rhodium might be the reason for activity improvement. In other words, the active sites for NO decomposition over 1 wt% Rh/CNTs are Rh^0. Similar to CNTs, the presence of H species enhanced the catalytic activity of the Rh/CNTs catalyst. For example, at 300 °C, totally 418.1 μl NO was converted in ten pulses of NO (totally 675 μl) over a 1 wt% Rh/CNTs sample pretreated (at 300 °C) with H_2 (table 2), whereas the corresponding amount was 67.5 μl over a fresh sample (figure 1). Over the H_2-treated (at 300 °C) 1 wt% Rh/CNTs sample, NO conversion decreased gradually to 21% with the rise in pulse number. Similar trend was observed over the samples pretreated at other H_2-reduction temperatures, respectively. It should be noted that the NO conversion (21%) in the tenth pulse was obviously higher than that (ca. 10%) observed over the fresh sample. TPR results suggested that Rh_2O_3 in Rh/CNTs could be reduced to Rh^0 at 280 °C (figure 7(b)). XPS investigation also showed that most of the rhodium in Rh/CNTs existed in the metallic form after being pretreated in H_2 at 300 °C for 1 h (figure 6). As indicated above, the H species in a CNTs catalyst react rather readily with NO; hence, the enhancement of NO conversion must be due to the presence of metallic rhodium and H species in the H_2-treated catalyst. From figure 4, one can note that the threshold temperature for CO_2 generation over 1 wt% Rh/CNTs is 400 °C. This observation suggests that in order to avoid the loss of carbon, the NO decomposition reaction has to be conducted below 400 °C. The CNTs material has gone through a calcination procedure of 500 °C in air for 2 h during preparation and is highly crystalline (figure 5). An important remark is: the CNTs support is more durable in NO oxidation than amorphous and fullerene carbons. García-García et al. [23] reported that activated carbon was involved in NO decomposition at 210 °C over 1 wt% Pt/activated carbon. In the forms of amorphous and fullerene, carbon can be oxidized to CO_2 in oxygen at temperatures above 500 °C [17,18].

Without H_2-pretreatment, the 1 wt% Rh/γ-Al_2O_3 catalyst showed poor catalytic activity for NO decomposition. XPS investigation illustrated that in a fresh sample, rhodium existed exclusively as Rh_2O_3 (figure 6). After H_2 reduction, the catalyst increased markedly in catalytic activity but was still inferior to Rh/CNTs in performance (table 2). For instance, after H_2-treatment at 300 °C, a total amount of 136.2 μl NO was converted in ten pulses of NO over Rh/γ-Al_2O_3, whereas the amount was 418.1 μl over Rh/CNTs. Similar trends were obtained over samples which were previously H_2-treated at other temperatures. The difference in activity could be better explained by the XPS results (figure 6). One can observe that the rhodium particles are heavily oxidized on γ-Al_2O_3, whereas on CNTs, it is not so. Therefore, the higher amount of metallic rhodium on Rh/CNTs is responsible for its higher activity. Generally speaking, the tendency of a metallic particle being oxidized increases with the decrease in particle size. Obviously, it is not the case for the Rh/CNTs and Rh/γ-Al_2O_3 catalysts. From table 1, it can be noted that the rhodium particle size was 10.7 nm for 1 wt% Rh/CNTs and 25.7 nm for 1 wt% Rh/γ-Al_2O_3. However, the former was less likely to be oxidized (figure 6). One possible explanation is that the strong interaction between metal and the CNTs support in Rh/CNTs hinders Rh from being oxidized. Even after H_2-treatment at 500 °C in air, 20% of the rhodium

in the Rh/CNTs catalyst was still in the metallic state; after the NO decomposition reaction, about 30% of rhodium was still metallic (figure 6). The relatively lower threshold temperature for H_2 reduction over 1 wt% Rh/CNTs as revealed in the TPR studies (figure 7) also suggested that the Rh_2O_3 on CNTs could be reduced more readily than that on γ-Al_2O_3.

5. Conclusion

The CNTs material showed moderate activity for NO decomposition. The loading of 1 wt% Rh on CNTs increased the catalytic activity greatly. The reduction of the catalyst by H_2 is beneficial for NO conversion. Compared to γ-Al_2O_3, CNTs is a better support material for rhodium dispersion and Rh^0 retention.

Acknowledgement

The work described above was fully supported by a grant from the Research Grants Council of the Hong Kong Special Administration Region, China (Project No. HKBU 2053/98P). We thank Professor B.L. Zhang of Chengdu Institute of Organic Chemistry, Chinese Academy of Sciences for performing the TEM investigation.

References

[1] M.S. Dresselhaus, G. Dresselhaus and P.C. Eklund, eds., *Science of Fullerenes and Carbon Nanotubes* (Academic Press, London, 1995).
[2] A.C. Dillon, K.M. Jones, T.A. Bekkedahl, C.H. Klang, D.S. Bethane and M.I. Heben, Nature (London) 386 (1997) 377.
[3] P. Chen, X. Wu, J. Lin and K.L. Tan, Science 285 (1999) 91.
[4] B. Coq, J.M. Planeix and V. Brotons, Appl. Catal. A 173 (1998) 175.
[5] J.M. Planeix, N. Coustel, B. Coq, V. Brotons, P.S. Kumbhar, R. Dutartre, P. Geneste, P. Bernier and P.M. Ajayan, J. Am. Chem. Soc. 116 (1994) 7935.
[6] Th. Braun, M. Wohlers, T. Belz, G. Nowizke, G. Wortmann, Y. Uchida, N. Pfänder and R. Schlögl, Catal. Lett. 43 (1997) 167.
[7] Th. Braun, M. Wohlers, T. Belz and R. Schlögl, Catal. Lett. 43 (1997) 175.
[8] J.C. Calvert, Pure Appl. Chem. 69 (1997) 1.
[9] V.I. Parvulescu, P. Grange and B. Delmon, Catal. Today 46 (1998) 233.
[10] M. Iwamoto, H. Furukawa, Y. Mine, F. Uemura, S. Mikuriya and S. Kagawa, J. Chem. Soc. Chem. Commun. (1986) 1272.
[11] A. Gervasini, P. Carniti and V. Ragaini, Appl. Catal. B 22 (1999) 201.
[12] A.M. Pisanu and C.E. Gigola, Appl. Catal. B 20 (1999) 179.
[13] S. Oh and C. Eickel, J. Catal. 128 (1991) 256.
[14] B. Cho, B. Shanks and J. Bailey, J. Catal. 115 (1989) 486.
[15] B. Cho, J. Catal. 148 (1994) 697.
[16] A.M. Pisanu and C.E. Gigola, Appl. Catal. B 20 (1999) 179.
[17] J.Z. Luo, Z.L. Yu, C.F. Ng and C.T. Au, J. Catal., submitted.
[18] K. Tohji, H. Takahashi, Y. Shinoda, N. Shimizu, B. Jeyadevon, I. Matsuoka, Y. Saito, A. Kasuya, S. Ito and Y. Nishina, J. Phys. Chem. B 101 (1997) 1974.
[19] *Handbook of X-Ray Photoelectron Spectroscopy* (Perkin–Elmer, Eden Prairie, MN).
[20] L.Z. Gao and C.T. Au, Catal. Lett. 65 (2000) 91.
[21] M. Rasinkangas, T.T. Pakkanen and T.A. Pakkanen, J. Organomet. Chem. 476 (1994) C6.
[22] M.J. Illán-Gómez, E. Raymundo-Pinero, A. García-García, A. Linares-Solano and C. Salinas-Martinez de Lecea, Appl. Catal. B 20 (1999) 267.
[23] A. García-García, M.J. Illán-Gómez, E. Raymundo-Pinero, A. Linares-Solano and C. Salinas-Martinez de Lecea, Appl. Catal. B 25 (2000) 39.